

Crossing constraints for hyperon reactions

Chueng-Ryong Ji and Stephen R. Cotanch

Department of Physics, North Carolina State University, Raleigh, North Carolina 27695

(Received 3 February 1988)

The importance and usefulness of crossing is emphasized for both kaon scattering and kaon production reactions. It is argued, and numerically demonstrated for a chiral Lagrangian, that crossing provides powerful, comprehensive constraints which are often neglected in the evaluation of dynamical models. Cross section calculations are presented for two distinct sets of crossing related reactions: (1) $K^-p \rightarrow K^-p$, $K^+p \rightarrow K^+p$ and $\bar{p}p \rightarrow K^-K^+$; (2) $K^-p \rightarrow \gamma\Lambda$ and $\gamma p \rightarrow K^+\Lambda$. The crossing relations require that the same hadronic Lagrangian, including coupling constants, govern all of these reactions, and results show that different reactions exhibit different sensitivity to coupling constant uncertainty. Because crossed reactions always entail different kinematic regions of the S matrix, it is expected that such sensitivity is not just representative of the current model but rather a general feature that should be exploited when investigating all relativistic theories.

I. INTRODUCTION

Crossing, first recognized in 1956¹ by Gell-Mann and Goldberger and developed by Gunson² and Olive,³ is a fundamental principle based on CPT and the analyticity of the S matrix. Even though no general proof exists (crossing has been rigorously demonstrated for "space" Lagrangian field theory), crossing has been elevated to the same status as the spin statistics and CPT theorems. Because of the connection to antiparticles crossing has been predominantly utilized in the field of particle physics,^{4,5} most notably in earlier and kaon scattering studies using dispersion relations (for typical pion and kaon applications see Refs. 6 and 7, respectively, and references therein). Now, in conjunction with the clear trend for new projects and accelerators dedicated to nuclear physics at higher energies, this principle should also be routinely incorporated in analyses conducted by the nuclear community.

The purpose of this paper is to stress the importance and usefulness of crossing in assessing dynamical models and in phenomenological studies. In particular, we find that channel crossing can reveal observable differences among model parameters which provide almost identical results in a certain channel. Thus our message is not only to simply avoid violating crossing, achieved by carefully and consistently using the same model (especially the same model parameters such as coupling constants) when describing crossed reactions, but also to advocate that crossing should be aggressively exploited by applying the model comprehensively to all crossed reactions that are observable. This will stringently test the model and provide full sensitivity to uncertainties in model parameters that might not be present in the analysis of a single isolated reaction. Even if the model uses running coupling constants, this statement should be correct when the magnitude of momentum transfer involved in crossed reactions is the same. As an example, the same form of quantum chromodynamic coupling constant $\alpha_s(|q^2|)$ can

be used both in timelike and spacelike regions of q^2 . This crossing constraint has not been widely appreciated in hyperon reactions.

This paper is organized into four sections. In Sec. II crossing relations and crossing symmetry are reviewed. These exact results, which are valid for any reaction, are applied to hyperon reactions since kaon scattering and production experiments are of current interest. Applications using a simple chiral quantum hydrodynamic Lagrangian are presented in Sec. III for the purely hadronic crossing related processes K^-p elastic, K^+p elastic and $\bar{p}p \rightarrow K^-K^+$. The electromagnetic crossed processes $\gamma p \rightarrow K^+\Lambda$ and $K^-p \rightarrow \gamma\Lambda$ are treated in Sec. IV using a more realistic Lagrangian which provides a reasonable description of the limited data. To our knowledge this is the first published cross section calculation for $K^-p \rightarrow \gamma\Lambda$, for which data is lacking, and we look forward to future experimental tests of our predictions. For each of the five reactions, cross sections, using different sets of coupling constants, are compared to reflect sensitivity to parameter uncertainty. In general, the degree of sensitivity to the same coupling constant uncertainty is different for different crossed channels. Finally, Sec. V summarizes and emphasizes the important issues and results.

II. CROSSING RELATIONS AND CROSSING SYMMETRY

Consider the general two-body $ab \rightarrow cd$ having scattering amplitude (S -matrix element) $S(p_a, p_b, p_c, p_d)$ where p_i represents the four-momentum for particle i and the order of variables, as it is throughout this paper, is important. Now consider the unphysical process $\bar{c}^*b \rightarrow \bar{a}^*d$, where the only change has been the crossing of particles a and c [change initial- (final-) state particle a (c) to final- (initial-) state antiparticle \bar{a} (\bar{c}) having opposite four-momentum $-p_a$ ($-p_c$) and sign-reversed additive quantum numbers, including spin magnetic substate].

The usual antiparticle notation is represented by the bar and the asterisk indicates unphysical four-momentum as now particles \bar{a}^* and \bar{c}^* both have negative total energy. The crossing hypothesis (more precisely CPT crossing component) asserts that this unphysical process is also mathematically described by the same amplitude $S(p_a, p_b, p_c, p_d)$ (i.e., the same complex number or the same complex function for variable four-momenta). Although interesting this result is not very useful. Now define a different S -matrix element $S'(p_{\bar{c}}, p_b, p_{\bar{a}}, p_d)$ to be the scattering amplitude for the physically allowed process $\bar{c}b \rightarrow \bar{a}d$ which only differs from the unphysical reaction above by the four-momentum of \bar{a} and \bar{c} [$p_{\bar{a}}$ and $p_{\bar{c}}$ are arbitrary but the energy of \bar{a} and \bar{c} are positive; all remaining reaction degrees of freedom, such as spin, remains the same so that again the additive quantum numbers have signs opposite to the original initial- (final-) state particle $a(c)$]. Crossing also requires that S' describe the unphysical crossed process $a^*b \rightarrow c^*d$ where now a^* and c^* have unphysical four-momentum $-p_{\bar{a}}$ and $-p_{\bar{c}}$. The crucial crossing assumption (distinct from CPT) is that the scattering amplitude is analytic so that complex continuation is possible in the momentum variables between the physical and unphysical regions. Then the original amplitude S , which describes the physical process $ab \rightarrow cd$, can be analytically continued to also describe the physical process $\bar{c}b \rightarrow \bar{a}d$. This result leads to the crossing relation

$$S'(p_{\bar{c}}, p_b, p_{\bar{a}}, p_d) = S(-p_{\bar{a}}, p_b, -p_{\bar{c}}, p_d), \quad (1)$$

which profoundly asserts that one and only one amplitude, in different regions of the complex plane, describes both of the above physical processes.

To further appreciate these points and to provide the conceptual framework for applications in the next two

sections it is useful to consider other crossings of the reaction $ab \rightarrow cd$. Including the original reaction there are a total of six different physical two-body reactions each having an amplitude that is related by crossing to the original amplitude $S(p_a, p_b, p_c, p_d)$. In Table I the six reactions are enumerated along with the corresponding labeled Mandelstam variables and physical amplitudes. Again an asterisk on a variable indicates evaluation in an unphysical kinematic region. There are no asterisks for reactions 1 and 6 because the former is an identity (no crossing) while the latter is equivalent to applying only CPT to reaction 1 and therefore does not require analytic continuation. Note also that because of CPT the crossing relations for reactions 2 and 5 are identical and similarly for reactions 3 and 4. Consequently, there are only two nontrivial crossing relations which can conveniently and uniquely be identified by the total energy variable in that channel. These are the t -channel crossing relation (reactions 3 and 4) involving $S(s^*, t^*, u)$ and the u -channel crossing relation (reactions 2 and 5) involving $S(s^*, t, u^*)$. It is also informative to mention the concept of crossing symmetry which is the mathematical symmetry of a specific amplitude under permutation of the Mandelstam variables. Crossing symmetry can be realized by specializing to reactions for which $\bar{c}=a$ or $\bar{d}=a$. The first yields the u -channel symmetry relation

$$S(s^*, t, u^*) = S(u, t, s), \quad (2)$$

representing symmetry under interchange of s and u (retaining the $*$ serves only to remind that all crossing and symmetry relations equate one physical and one unphysical amplitude). The second special reaction, $\bar{d}=a$, generates the t -channel symmetry relation

$$S(s^*, t^*, u) = S(t, s, u), \quad (3)$$

TABLE I. Mandelstam variables and crossing relations for the reaction $ab \rightarrow cd$. An asterisk indicates an unphysical kinematic value.

Reaction	Mandelstam variables	Crossing relation
1. $ab \rightarrow cd$ s channel	$s_1 = (p_a + p_b)^2 \equiv s$ $t_1 = (p_c - p_a)^2 \equiv t$ $u_1 = (p_d - p_a)^2 \equiv u$	$S_1(s_1, t_1, u_1) = S(s, t, u)$ $= S(s_1, t_1, u_1)$
2. $\bar{c}b \rightarrow \bar{a}d$ u channel	$s_2 = (p_{\bar{c}} + p_b)^2 = u^*$ $t_2 = (p_{\bar{a}} - p_{\bar{c}})^2 = t$ $u_2 = (p_d - p_{\bar{c}})^2 = s^*$	$S_2(s_2, t_2, u_2) = S(s^*, t, u^*)$ $= S(u_2, t_2, s_2)$
3. $\bar{d}b \rightarrow \bar{c}a$ t channel	$s_3 = (p_{\bar{d}} + p_b)^2 = t^*$ $t_3 = (p_c - p_{\bar{d}})^2 = s^*$ $u_3 = (p_a - p_{\bar{d}})^2 = u$	$S_3(s_3, t_3, u_3) = S(s^*, t^*, u)$ $= S(t_3, s_3, u_3)$
4. $a\bar{c} \rightarrow \bar{b}d$ t channel	$s_4 = (p_a + p_{\bar{c}})^2 = t^*$ $t_4 = (p_{\bar{b}} - p_a)^2 = s^*$ $u_4 = (p_d - p_a)^2 = u$	$S_4(s_4, t_4, u_4) = S(s^*, t^*, u)$ CPT equivalent to 3
5. $a\bar{d} \rightarrow \bar{c}b$ u channel	$s_5 = (p_a + p_{\bar{d}})^2 = u^*$ $t_5 = (p_{\bar{c}} - p_{\bar{d}})^2 = t$ $u_5 = (p_b - p_{\bar{d}})^2 = s^*$	$S_5(s_5, t_5, u_5) = S(s^*, t, u^*)$ CPT equivalent to 2
6. $\bar{c}\bar{d} \rightarrow \bar{a}\bar{b}$ s channel	$s_6 = (p_{\bar{c}} + p_{\bar{d}})^2 = s$ $t_6 = (p_a - p_{\bar{c}})^2 = t$ $u_6 = (p_{\bar{b}} - p_{\bar{c}})^2 = u$	$S_6(s_6, t_6, u_6) = S(s, t, u)$ CPT equivalent to 1

which indicates symmetry under interchange of s and t .

Finally, the Lorentz-invariant transition amplitude T has the same crossing properties as S and is related to the invariant S matrix by

$$S_{fi} = (\rho_a \rho_b \rho_c \rho_d)^{1/2} \delta_{fi} + i(2\pi)^4 \delta(p_f - p_i) T_{fi}. \quad (4)$$

Here δ_{fi} contains Dirac and Kronecker delta functions representing the preservation of the initial state in the absence of scattering interactions with the coefficient determined by the covariant normalization choice for single-particle state:

$$\langle \mathbf{p}_x | \mathbf{p}'_x \rangle = (2\pi)^3 n_x E_x \delta(\mathbf{p}_x - \mathbf{p}'_x) \equiv \rho_x \delta(\mathbf{p}_x - \mathbf{p}'_x), \quad (5)$$

$$n_x = \frac{1}{m_x} \text{ fermions mass } m_x \quad (6)$$

$$= 2 \text{ bosons or fermions mass } 0. \quad (7)$$

The initial, final total four-momentum is represented by p_i, p_f and E_x is the total energy of particle x . The invariant cross section element, which is not directly constrained by crossing, is given by

$$d\sigma = \frac{(2\pi)^4}{n_a n_b F} |T_{fi}|^2 \delta(p_f - p_i) \frac{d\mathbf{p}_c}{\rho_c} \frac{d\mathbf{p}_d}{\rho_d}, \quad (8)$$

where $d\mathbf{p}_x$ is the three-momentum of particle x and F is the invariant flux factor

$$F = [(p_a \cdot p_b)^2 - p_a^2 p_b^2]^{1/2} \quad (9)$$

(if c and d are identical particles the cross section must also be divided by 2).

Summarizing this section, crossing is a profound result which is postulated to be an absolute principle, independent of physical dynamics, based on analyticity and the equivalence between initial- (final-) state particle with four-momentum p and final- (initial-) state antiparticle with $-p$ (CPT invariance). It is a property which all relativistic scattering amplitudes, derived from sophisticated or simple models, must reflect.

With these preliminaries we now apply our results to hadronic and electromagnetic reactions involving hyperons. Our emphasis will not be on the physics but rather the usefulness and significance of crossing in the investigation of dynamic theories.

III. CROSSING FOR HYPERON HADRONIC PROCESSES

For a clear example we now consider the specific case where $a = c = K^-$ and $b = d = p$. From the previous section we expect that the u -channel crossing relation will generate the $K^+ p$ elastic scattering amplitude (this will be reaction 2 in Table I) and that the t -channel crossing relation will provide the $\bar{p} p \rightarrow K^- K^+$ amplitude (reaction 3). We therefore only need to focus on generating the s -channel $K^- p$ elastic amplitude (reaction 1) which will require a dynamic model. Because our thrust concerns illustrating the significance of crossing we adopt a simple model—a chiral Lagrangian based on quantum hydrodynamics (quantum field theory involving mesons, baryons but no explicit color degrees of freedom). We re-

strict this application to low energies (i.e., 1 GeV or less) and therefore only introduce free fields for the lightest particles which are believed to be most important. These are the isospin singlet Λ , doublets N, K and triplet Σ :

$$N = \begin{bmatrix} p \\ n \end{bmatrix}, \quad K = \begin{bmatrix} K^+ \\ K^0 \end{bmatrix},$$

$$\Sigma = (\Sigma_1, \Sigma_2, \Sigma_3), \quad \Sigma^\pm = \frac{\mp \Sigma_1 + i \Sigma_2}{\sqrt{2}}, \quad \Sigma^0 = \Sigma_3,$$

with corresponding antiparticle fields

$$\bar{N} = (\bar{p}, \bar{n}), \quad \bar{K} = (K^-, \bar{K}^0),$$

$$\bar{\Sigma} = (\bar{\Sigma}_1, \bar{\Sigma}_2, \bar{\Sigma}_3), \quad \bar{\Sigma}^\pm = \frac{\mp \bar{\Sigma}_1 - i \bar{\Sigma}_2}{\sqrt{2}}, \quad \bar{\Sigma}^0 = \bar{\Sigma}_3,$$

involving the usual adjoint notation for fermion fields (e.g., $\bar{p} = p^+ \gamma_0$). The hermitian interaction Lagrangian \mathcal{L}_I is taken to be pseudoscalar coupling with two phenomenological coupling constants g_Λ and g_Σ :

$$\begin{aligned} \mathcal{L}_I = & ig_\Lambda [\bar{N} \gamma_5 \Lambda K + \bar{K} \bar{\Lambda} \gamma_5 N] \\ & + ig_\Sigma [\bar{N} \gamma_5 \tau \cdot \Sigma K + \bar{K} \bar{\Sigma} \cdot \tau \gamma_5 N]. \end{aligned} \quad (10)$$

Here γ_5 and γ_0 are the familiar Dirac matrices and τ represents the isospin Pauli matrices. We refer to our approach as a chiral Lagrangian model because of the presence of the chiral operator γ_5 in Eq. (10) and note that because of mass terms in the unperturbed Lagrangian overall chiral symmetry is not preserved. Related, pseudovector coupling, which is mandated for the pion to retain consistency with low-energy theorems and partial conservation of axial-vector current (PCAC), is not necessarily required for the kaon system because of the more severe chiral-symmetry breaking associated with the kaon's much heavier mass.

The invariant scattering amplitude, introduced in Sec. II, can be expressed in most general form in terms of two elementary amplitudes A and B which are Lorentz scalar:

$$T_{\lambda\lambda'}^S(q, p, q', p') = \bar{u}(p', \lambda') \left[A_s + \left[\frac{\not{q} + \not{q}'}{2} \right] B_s \right] u(p, \lambda), \quad (11)$$

where \not{q} is the Feynmann slash, $\not{q} = \gamma \cdot q$, and $u(p, \lambda)$ is the standard Dirac spinor with four-momentum p , helicity λ and normalization specified by

$$\bar{u}(p, \lambda') u(p, \lambda) = \delta_{\lambda\lambda'}. \quad (12)$$

For notational simplicity we have represented the proton and kaon four-momentum by p and q , respectively (primes indicate final-state quantities). Using diagrammatic techniques we have computed the elementary amplitudes to second order in the coupling constants yielding

$$A_s = \sum_{Y=\Lambda, \Sigma^0} \frac{g_Y^2}{s - m_Y^2} (m_Y - m_p), \quad (13)$$

$$B_s = - \sum_{Y=\Lambda, \Sigma^0} \frac{g_Y^2}{s - m_Y^2}. \quad (14)$$

Note that A and B only depend on $s=(q+p)^2$ and not $t=(q'-q)^2$ or $u=(p'-q)^2$. Utilizing Eq. (8) and averaging over the proton helicities, the center-of-momentum unpolarized cross section is given by

$$\frac{d\sigma^s}{d\Omega} = \frac{1}{2} \left[\frac{m_p}{4\pi W} \right]^2 \sum_{\lambda\lambda'} |T_{\lambda\lambda'}^s|^2, \quad (15)$$

where $W=\sqrt{s}$ is the total center-of-momentum (c.m.) energy. Performing the spin summations produces the final result

$$\frac{d\sigma^s}{d\Omega} = f_1^2 + f_2^2 + 2f_1 f_2 \cos\theta, \quad (16)$$

with

$$f_1 = \frac{m_p + E_p}{8\pi W} [A_s + (W - m_p)B_s], \quad (17)$$

$$f_2 = \frac{m_p - E_p}{8\pi W} [A_s - (W + m_p)B_s]. \quad (18)$$

We have investigated the sensitivity of the K^-p elastic cross section to the uncertainty in the Λ and Σ coupling constants. In Fig. 1 we summarize our results by presenting three curves corresponding to three different coupling constant sets listed in Table II. These sets, labeled A (Ref. 8), B (Ref. 8), and C (Ref. 9), were obtained from kaon photoproduction phenomenological analyses and will also be used in the next section that addresses crossing for electromagnetic hyperon processes. Only the first

two columns are relevant to the hadronic calculations reported in this section. Because of the simplicity of our model it is not surprising that none of the theoretical curves quantitatively describes the data¹⁰ also shown in Fig. 1. The K^-p system, even at threshold, has several effects such as coupling to other open channels ($\Lambda\pi$ and $\Sigma\pi$) and excited hyperon states (Λ^* and Σ^*), especially $\Lambda(1405)$ and $\Lambda(1520)$ which are known to be important. These have not been included because, as emphasized earlier, our thrust here is to document the utility of crossing in constraining dynamic model analysis. The key issue is that different channels (s , t , or u) may reveal different and useful sensitivity to the same underlying model parameters. The simple Coulomb amplitude has also been omitted. We have therefore focused on back angles, where this amplitude is unimportant, for s - and u -channel elastic scattering. With this in mind we now address the u -channel K^+p elastic and t -channel $\bar{p}p \rightarrow K^-K^+$ processes to determine their sensitivity to the same three sets of coupling constants.

The K^+p cross section has the same phase space as K^-p so Eq. (15) represents the differential cross section provided the K^+p u -channel amplitude, T^u , is used. This amplitude can be evaluated from first principles (which we have also done to explicitly confirm crossing) or by simply applying crossing. Crossing, actually substitution in this case, specifies that the K^+p amplitude, $T^u(q_2, p_2, q'_2, p'_2)$ (2 indicates u -channel variables), is simply given by the K^-p amplitude evaluated in the unphysical region

$$T_{\lambda\lambda'}^u(q_2, p_2, q'_2, p'_2) = T_{\lambda\lambda'}^s(-q_2, p_2, -q'_2, p'_2), \quad (19)$$

or since $s_2 = u$, $t_2 = t$, and $u_2 = s$ and by definition

$$T_{\lambda\lambda'}^u(q_2, p_2, q'_2, p'_2) = \bar{u}(p'_2, \lambda') \left[A_u(s_2, t_2, u_2) + \left(\frac{q_2 + q'_2}{2} \right) B_u(s_2, t_2, u_2) \right] u(p_2, \lambda), \quad (20)$$

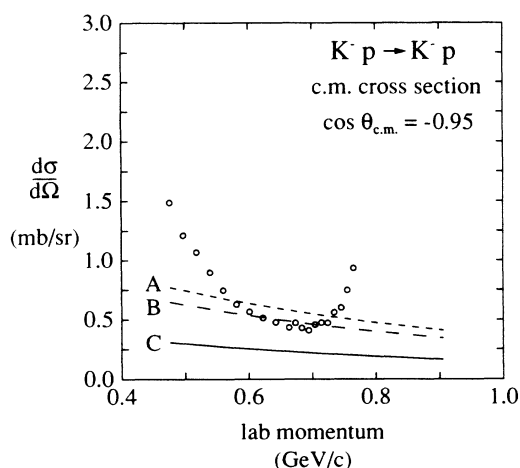


FIG. 1. Theoretical and experimental (Ref. 10) (circles, error bars are omitted) K^-p elastic scattering cross sections. The different theoretical curves correspond to the three sets of coupling constants A (short dashed), B (long dashed), and C (solid) listed in Table II. Only the first two columns of Table II are used for the calculations displayed in Figs. 1–3.

we immediately have the crossing relations for the elementary amplitudes which complete the K^+p calculation:

$$\begin{aligned} A_u(s_2, t_2, u_2) &= A_s(u_2, t_2, s_2) \\ &= \sum_Y \frac{g_Y^2}{u_2 - m_Y^2} (m_Y - m_p), \end{aligned} \quad (21)$$

TABLE II. Different sets of coupling constants. The first two columns are used in Sec. II for the purely hadronic calculations, while all four columns are used in Sec. IV for the electromagnetic applications. Note that the Σ coupling constant, g_Σ , was determined from $G_\Sigma = k_T g_\Sigma$ where G_Σ is given in Refs. 8 and 9 and $k_T = -2.24$ is the dimensionless Λ - Σ transition moment factor.

Set	$\frac{g_\Lambda}{\sqrt{4\pi}}$	$\frac{g_\Sigma}{\sqrt{4\pi}}$	$\frac{G_Y}{4\pi}$	$\frac{G_T}{4\pi}$
A (Ref. 8)	2.57	-0.679	0.105	0.064
B (Ref. 8)	2.49	-0.518	0.226	-0.062
C (Ref. 9)	2.04	0.554	0.247	-0.189

$$B_u(s_2, t_2, u_2) = -B_s(u_2, t_2, s_2) = \sum_Y \frac{g_Y^2}{u_2 - m_Y^2}. \quad (22)$$

Equations (16)–(18) again specify the cross section with $W = \sqrt{s_2}$.

Figure 2 summarizes our sensitivity study for K^+p elastic scattering. Again the same three sets of coupling constants are used. Notice that the sensitivity is somewhat different than that reflected by K^-p scattering in Fig. 1. Also notice that this simple theoretical approach provides a more quantitative description of the data.¹¹ This is predominantly because there are no known strangeness +1 baryons. Hence strangeness conservation restricts KN scattering to elastic and simple charge exchange (effective single-channel phenomena). Further, strangeness -1 baryons only contribute in the s (s_1) channel for $\bar{K}N$ and the u (u_2) channel for KN . Since $s_1 > 0$ and $u_2 < 0$, Eqs. (13), (14), (21), and (22) indicate the $\bar{K}N$ cross section will have significantly more variation with energy (i.e., the well-known result that the cross section is dominated by s -channel poles).

Our final purely hadronic application is to t -channel crossing to describe the reaction $\bar{p}p \rightarrow K^-K^+$. The physical kinematics are now p_3 for \bar{p} , p_3 for p , q_3' for K^+ , and q_3' for K^- . Then, under crossing,

$$T_{\lambda\bar{\lambda}}^t(p_3, p_3, q_3', q_3') = \bar{v}(p_3, \bar{\lambda}) \left[A_s(t_3, s_3, u_3) + \left[\frac{-q_3' + q_3'}{2} \right] B_s(t_3, s_3, u_3) \right] u(p_3, \lambda), \quad (24)$$

where now $s_3 = t$, $t_3 = s$, and $u_3 = u$. The elementary amplitudes are still given by Eqs. (13) and (14). We have also evaluated this process from first principles to verify Eq. (24) and confirm the elementary amplitude crossing relations

$$A_t(s_3, t_3, u_3) = A_s(t_3, s_3, u_3) = \sum_Y \frac{g_Y^2}{t_3 - m_Y^2} (m_Y - m_p), \quad (25)$$

$$B_t(s_3, t_3, u_3) = -B_s(t_3, s_3, u_3) = \sum_Y \frac{g_Y^2}{t_3 - m_Y^2}. \quad (26)$$

Because the phase space is different Eq. (15) no longer applies. Using Eq. (8) directly yields for the spin-averaged c.m. cross section

$$\frac{d\sigma^t}{d\Omega} = \frac{1}{4s_3} \left[\frac{m_p^2}{4\pi} \right]^2 \left[\frac{s_3 - 4m_K^2}{s_3 - 4m_p^2} \right]^{1/2} \sum_{\lambda\bar{\lambda}} |T_{\lambda\bar{\lambda}}^t|^2, \quad (27)$$

with

$$\sum_{\lambda\bar{\lambda}} |T_{\lambda\bar{\lambda}}^t|^2 = \frac{1}{8m_p^2} \{ s_3 [4A_t^2 + (s_3 - 4m_K^2)B_t^2] - [(4m_p A_t + (t_3 - u_3)B_t)^2] \}. \quad (28)$$

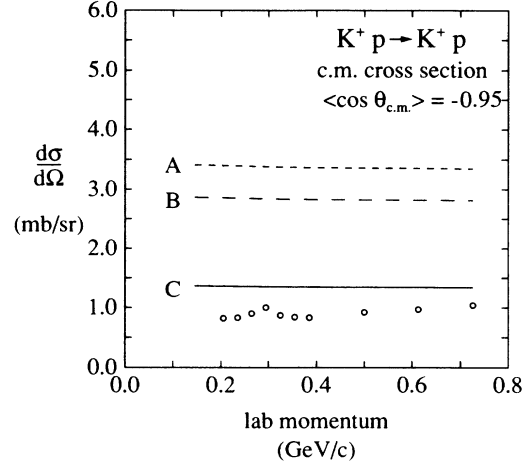


FIG. 2. Same as Fig. 1 for K^+p elastic scattering. Data from Ref. 11.

$$T_{\lambda\bar{\lambda}}^t(p_3, p_3, q_3', q_3') = T_{\lambda-\bar{\lambda}}^s(-q_3', p_3, q_3', -p_3), \quad (23)$$

where, as mentioned previously, the order of the arguments is important. Using Eq. (11) we can easily evaluate this result, provided we replace $\bar{u}(-\bar{p}, -\bar{\lambda})$ by $\bar{v}(\bar{p}, \bar{\lambda})$ (which follows by definition):

Figure 3 displays our sensitivity study for $\bar{p}p \rightarrow K^-K^+$ for the same three sets of coupling constants. Comparing Figs. 1, 2, and 3 further supports our claim that the sensitivity to model parameters is different for different channels. Our calculated cross sections are larger than experiment¹² by an order of magnitude at forward angles and roughly 2 orders of magnitude at backward angles (not

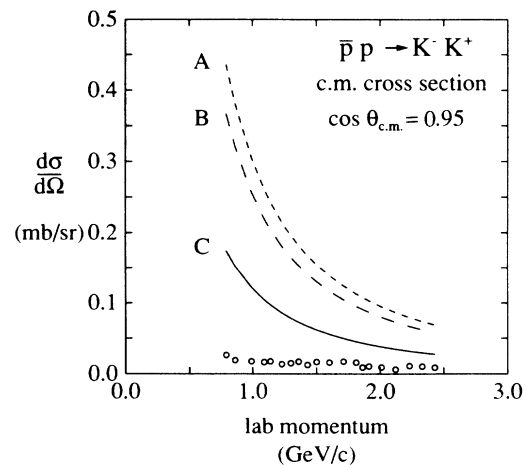


FIG. 3. Same as Fig. 1 for $\bar{p}p \rightarrow K^-K^+$. Data from Ref. 12.

shown) which represents the clear inadequacy of the simple Born terms. Because the Born amplitudes are real they violate unitarity, a constraint which is very important for inelastic processes. Reference 13 discusses this point further and presents a more accurate description of $\bar{p}p \rightarrow K^- K^+$.

IV. CROSSING FOR HYPERON ELECTROMAGNETIC PROCESSES

We now apply our results to electromagnetic reactions and document the sensitivity of calculations for kaon photoproduction, $\gamma p \rightarrow K^+ \Lambda$, and kaon radiative capture, $K^- p \rightarrow \gamma \Lambda$, to the full set of coupling constants listed in Table II. Because new, improved measurements are planned for these processes [at Continuous Electron Beam Accelerator Facility (CEBAF), Japan's National Laboratory for High Energy Physics (KEK), and proposed North American "kaon factories"] and because these reactions entail electromagnetic coupling ($e^2/4\pi \simeq 1/137$), which is more amenable to our perturbative treatment we have been motivated to include additional refinements. As demonstrated in Refs. 8 and 14 a more realistic theoretical treatment can be obtained by extending the model to accommodate vector meson K^* exchange.

The purely hadronic interaction Lagrangian is now generalized to describe K^* exchange by adding

$$\mathcal{L}_I^{K^*} = \mathcal{L}_I^V + \mathcal{L}_I^T, \quad (29)$$

where \mathcal{L}_I^V and \mathcal{L}_I^T are the vector and tensor interactions involving respective coupling constants $g_{K^*}^V$ and $g_{K^*}^T$:

$$\mathcal{L}_I^V = -ig_{K^*}^V (\bar{N} \gamma^\mu \Lambda K_\mu^* + \bar{K}_\mu^* \bar{\Lambda} \gamma^\mu N), \quad (30)$$

$$\mathcal{L}_I^T = -\frac{ig_{K^*}^T}{m_p + m_\Lambda} [\bar{N} \sigma^{\mu\nu} \Lambda (\nabla_\mu K_\nu^* - \nabla_\nu K_\mu^*) + (\nabla_\mu \bar{K}_\nu^* - \nabla_\nu \bar{K}_\mu^*) \bar{\Lambda} \sigma^{\mu\nu} N]. \quad (31)$$

Here K_μ^* represents the vector kaon field which is an isospin doublet (we use the same isospin notation as for K defined previously), ∇_μ is the standard four-gradient and $\sigma^{\mu\nu}$ is defined by

$$\sigma^{\mu\nu} = \frac{i}{2} (\gamma^\mu \gamma^\nu - \gamma^\nu \gamma^\mu). \quad (32)$$

We now introduce the photon field A_μ with field strength tensor $F_{\mu\nu}$

$$F_{\mu\nu} = \nabla_\mu A_\nu - \nabla_\nu A_\mu. \quad (33)$$

The presence of this field leads to the following electromagnetic interaction Lagrangian $\mathcal{L}_I^{\text{em}}$ which must be added to the Lagrangians specified by Eqs. (10) and (29):

$$\begin{aligned} \mathcal{L}_I^{\text{em}} = & -e(J_p^\mu + J_K^\mu) A_\mu \\ & -(\mu_p \bar{p} \sigma^{\mu\nu} p + \mu_\Lambda \bar{\Lambda} \sigma^{\mu\nu} \Lambda + \mu_T \bar{\Lambda} \sigma^{\mu\nu} \Sigma^0) F_{\mu\nu} \\ & -\frac{g_{KK^*}^\gamma}{m} \varepsilon^{\alpha\beta\gamma\delta} [K^+ \nabla_\alpha K_\beta^{*+} + K^- \nabla_\alpha K_\beta^{*-}] \nabla_\gamma A_\delta, \end{aligned} \quad (34)$$

where m is a mass, arbitrarily taken to be 1 GeV, introduced to make the K^*-K electromagnetic coupling constant, $g_{KK^*}^\gamma$, dimensionless. The current J^μ and anomalous magnetic moments μ are given by

$$J_p^\mu = \bar{p} \gamma^\mu p \quad (\text{proton current}), \quad (35)$$

$$J_K^\mu = i(K^- \nabla^\mu K^+ - K^+ \nabla^\mu K^-) \quad (\text{kaon current}), \quad (36)$$

$$\mu_p = \frac{\kappa_p e}{2m_p} \quad (\text{proton moment}), \quad (37)$$

$$\mu_\Lambda = \frac{\kappa_\Lambda e}{2m_\Lambda} \quad (\Lambda \text{ moment}), \quad (38)$$

$$\mu_T = \frac{\kappa_T e}{m_\Lambda + m_{\Sigma^0}} \quad (\Sigma^0 \rightarrow \Lambda \text{ transition moment}). \quad (39)$$

From experiment, $\kappa_p = 1.79$, $\kappa_\Lambda = -0.73$, and $\kappa_T = -2.24$ (magnitude determined from the 5.8×10^{-20} s lifetime for $\Sigma^0 \rightarrow \Lambda \gamma$; sign is inferred from the quark model).

We now apply these results beginning with K^+ photoproduction, $\gamma p \rightarrow K^+ \Lambda$, which we take to be the s channel. For clarity, in this section we denote the γ , p , K^+ , and Λ four-momenta by q , p , k , and l and the γ , p , and Λ helicities by h , λ , and λ' , respectively. Because the photon has unit spin, described by the polarization four-vector $\varepsilon_\mu(q, h)$ the invariant transition matrix element $T_{h\lambda\lambda'}^s$ now contains four elementary amplitudes, A_i :

$$T_{h\lambda\lambda'}^s(q, p, k, l) = \bar{u}(l, \lambda') \gamma_5 \varepsilon_\mu(q, h) N_l^\mu A_i^s u(p, \lambda), \quad (40)$$

with bilinear four-vectors N_l^μ given by

$$N_1^\mu = -\gamma^\mu \not{q}, \quad (41)$$

$$N_2^\mu = 2(p^\mu q \cdot l - l^\mu q \cdot p), \quad (42)$$

$$N_3^\mu = \gamma^\mu q \cdot p - p^\mu \not{q}, \quad (43)$$

$$N_4^\mu = \gamma^\mu q \cdot l - l^\mu \not{q}. \quad (44)$$

As reported in a previous study¹⁴ we have calculated the elementary amplitudes by evaluating the S matrix to second order for the above Lagrangian. These amplitudes, which are summarized in the Appendix, are functions of $s = (q + p)^2$, $t = (k - q)^2$, $u = (l - q)^2$, and the coupling constants which conveniently group into the effective parameters

$$G_\Sigma = \kappa_T g_\Sigma, \quad (45)$$

$$G_V = g_{KK^*}^\gamma * g_{K^*}^V, \quad (46)$$

$$G_T = g_{KK^*}^\gamma * g_{K^*}^T, \quad (47)$$

which, along with g_Λ , have been phenomenologically analyzed previously^{8,9} and are listed in Table II. From Eq. (8) the spin-averaged c.m. cross section is

$$\frac{d\sigma^s}{d\Omega} = \frac{1}{4} \frac{m_p m_\Lambda}{(4\pi W)^2} \frac{|\mathbf{k}|}{|\mathbf{q}|} \sum_{h\lambda\lambda'} |T_{h\lambda\lambda'}^s|^2, \quad (48)$$

where \mathbf{k} , \mathbf{q} are the kaon, photon c.m. momentum. Using trace techniques and computer algebra, Eq. (48) has been reduced and is specified in the Appendix.

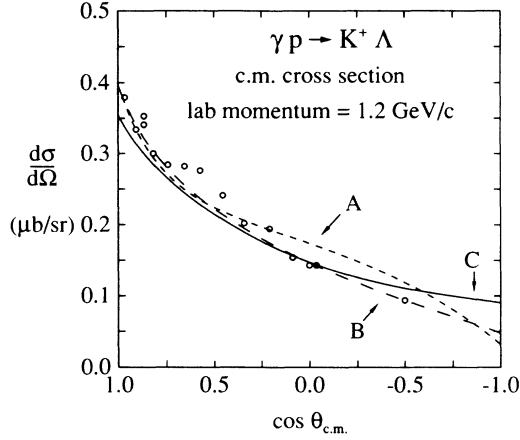


FIG. 4. Same as Fig. 1 for $\gamma p \rightarrow K^+ \Lambda$. All four columns of coupling constants in Table II are used for the calculations displayed in Figs. 4 and 5. Data from Ref. 15.

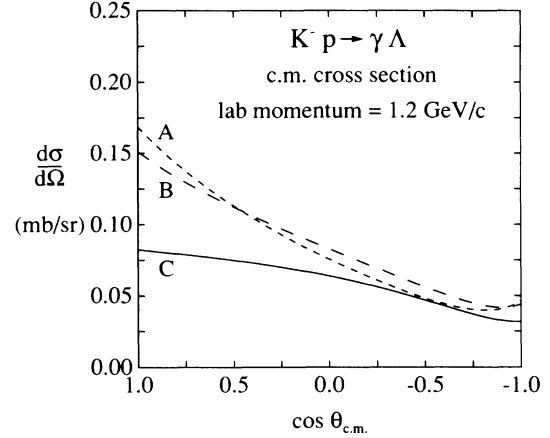


FIG. 5. Same as Fig. 4, without data, for $K^- p \rightarrow \gamma \Lambda$.

In Fig. 4 we display the photoproduction cross sections corresponding to the three sets of coupling constants in Table II. All curves provide a reasonable description of the data.¹⁵ This is expected since each set was phenomenologically determined using this reaction. Again, our major thrust in this paper is not the physics of this reaction but to demonstrate that crossing can provide a powerful criterion for determining model completeness as parameters appropriately describing one channel may or may not provide a consistent description of crossed channels.

We now address the u -channel process $K^- p \rightarrow \gamma \Lambda$. Crossing the photon and kaon in the s channel gives the, by now ubiquitous, relations for the physical u channel having kaon momentum \bar{k} , photon momentum \bar{q} , photon helicity \bar{h} :

$$T_{\bar{h}\lambda\lambda'}^u(\bar{k}, p, \bar{q}, l) = T_{-\bar{h}\lambda\lambda'}^s(-\bar{q}, p, -\bar{k}, l), \quad (49)$$

$$T_{\bar{h}\lambda\lambda'}^u(\bar{k}, p, \bar{q}, l) = \bar{u}(l, \lambda') \gamma_5 \epsilon_\mu(\bar{q}, \bar{h}) \times N_i^\mu A_i^\mu(s_2, t_2, u_2) u(p, \lambda), \quad (50)$$

where the N_i^μ are again functionally specified by Eqs. (41)–(44). Equating Eqs. (49) and (50) gives the crossing relations for the elementary amplitudes

$$A_i^\mu(s_2, t_2, u_2) = -A_i^s(u_2, t_2, s_2), \quad i=1, 2, 3, 4, \quad (51)$$

with change sign under $s_1 \rightarrow u_2$ and $u_1 \rightarrow s_2$ because the four-vectors N_i^μ also change for $q \rightarrow -\bar{q}$. We have confirmed these results through detailed diagrammatic calculations. Accordingly, Eq. (51), when combined with the Appendix, completely determines the amplitudes. From Eq. (8) the spin-averaged c.m. cross section is

$$\frac{d\sigma^\mu}{d\Omega} = \frac{1}{2} \frac{m_p m_\Lambda}{(4\pi W)^2} \frac{|\bar{q}|}{|\bar{k}|} \sum_{\bar{h}\lambda\lambda'} |T_{\bar{h}\lambda\lambda'}^u|^2, \quad (52)$$

where W is the $K^- p$ c.m. total energy and \bar{k}, \bar{q} are the kaon, photon c.m. three-momenta, respectively. The

spin-averaged transition probability is specified in the Appendix.

In Fig. 5 we present our final sensitivity comparison. The significant result is that within the framework of a more sophisticated model, channel crossing again reveals informative differences among coupling constant sets which provide almost identical s -channel results. Unfortunately, there is very limited data for this reaction, as it would be interesting to see which phenomenological set, if any, would be favored. This represents a promising experiment for KEK and other proposed “kaon factories.”

While cross section angular distributions are not available the branching ratio for $K^- p \rightarrow \gamma \Lambda$ has been measured¹⁶ to be within the range $(2.8 \pm 0.8) \times 10^{-3}$. We have calculated this observable for each coupling constant set and obtained the values: set A, 1.82×10^{-3} ; set B, 1.68×10^{-3} ; set C, 9.83×10^{-4} . Notice that again crossing reveals parameter sensitivity and that the value provided by set A is near the lower experimental range. A more detailed theoretical treatment for this branching ratio has recently been published.¹⁷ This work reports $K^- p \rightarrow \gamma \Lambda$ calculations for a $K^- p$ atomic initial configuration and also presents results from including additional diagrams corresponding to various N^* and Y^* exchanges. Although Ref. 17 computed branching ratios within the experimental range, their coupling constants were determined by kaon-induced hadronic processes which, as we have explicitly confirmed, do not reproduce kaon photoproduction data. This shortcoming, the inability to simultaneously describe both hadronic and electromagnetic processes involving kaons, has been noted earlier¹⁸ and is most likely due to the model simplicity. As stated earlier in this paper, a perturbative, phenomenological Lagrangian approach that explicitly includes only a few mesons and baryons is incomplete and for purely hadronic processes is probably incapable of providing a detailed description. Even for $K^+ p$ scattering, which is significantly constrained and simplified by strangeness conservation, there are several meson ex-

change contributions which, as examined in Ref. 19, are important and should be consistently included. Again, our thrust in this paper is not to advocate or critique a particular dynamic approach but rather to demonstrate the utility of crossing for the development of improved, realistic models, a topic we are currently investigating.

Recently other, more detailed phenomenological studies (see models in Refs. 9 and 16) have been reported for $\gamma p \rightarrow K^+ \Lambda$ involving the additional exchanges from several N^* resonances. Their extracted coupling constants differ markedly from Table II. We have performed $\gamma p \rightarrow K^+ \Lambda$ and $K^- p \rightarrow \gamma \Lambda$ calculations for these coupling constant sets (actually just a four-parameter subset corresponding to our model) but do not show results because such calculations inconsistently use parameters appropriate to a more extended model. However, we again find significant differences in sensitivity for different channels.

Because the prospects for t -channel measurements are not good (secondary beams could permit study of $\bar{\Lambda} p \rightarrow \gamma K^+$) we do not present crossing relation results for this channel. These can be easily generated from the above equations.

V. CONCLUSION

In this paper we have presented a pedagogical discussion of crossing, demonstrated the practicality of crossing for generating amplitudes in the t and u channels without recourse to dynamic calculations, calculated the first crossing consistent prediction for $K^- p \rightarrow \gamma \Lambda$, and, most significantly, shown the utility of crossing for revealing different model sensitivity in different crossed channels. Our major contribution has been to further demonstrate that this sensitivity is not related to a particular class of reactions nor to the level of sophistication of dynamic models. We submit this is a general result which will be present, to a greater or lesser extent, in any analysis.

Because this paper focused on crossing applications involving simple algebraic forms for the transition amplitude, crossed channel amplitudes were particularly easy to generate (just substitution). It is important to stress that crossing can also be practically applied to more complicated analyses involving numerical representation for the amplitudes and may provide a more convenient, refined alternative.²⁰ For example, provided analyticity is maintained, coupled-channel calculations for $\Lambda p \rightarrow \Lambda p$ scattering²¹ could, in principle, be used for $\bar{p} p \rightarrow \Lambda \Lambda$ with no need for introducing complex phenomenological potentials (other than a complex propagator arising from the decay width of an exchange particle having finite lifetime) describing annihilation. By using interactions derived from field theory which describe multiple π , ρ , and ω exchange, one could gain significant insight into the $\bar{p} p$ annihilation mechanism (roughly 20% of the low-energy $\bar{p} p$ total annihilation cross section is due to the $\bar{p} p \rightarrow \pi^+ \pi^- \pi^+ \pi^- \pi^0$ channel which is known to couple strongly to the $\bar{p} p \rightarrow \rho^0 \omega$ process²²). Even though one complete Lagrangian governs both Λp scattering and $\bar{p} p$ reactions, as indicated in this paper these two processes may indeed reveal entirely different sensitivity to various

Lagrangian components and higher-order diagram subsets. In this case a realistic Λp model calculation may, when crossed, predict unsatisfactory $\bar{p} p$ results. This would still provide important insight and help identify the dynamic aspects which should be further investigated. In turn, coupled-channel $\bar{p} p$ calculations, which have recently been reported,²³ should also be crossed for Λp predictions. Ultimately, with the aid of crossing, one self-consistent reaction model (or two mutually consistent models if the reactions are almost dynamically independent) would evolve for comprehensively describing both Λp and $\bar{p} p$ processes. A major difficulty, however, is that nonrelativistic potential scattering theory generates S -matrix amplitudes with analyticity domains restricted to the physical region (i.e., total particle energy, including rest mass, is positive-definite). Crossing relations only exist for theories which can properly incorporate particles having both positive and negative total energy. Accordingly and at a minimum, a relativistic coupled-channel formalism is necessary. We have initiated such studies and will report results in a future communication.

In summary, crossing is an exact, powerful property of the S matrix that provides useful theoretical constraints. Violations of this principle, which can occur in uncaredful analyses that incorrectly regard the s , t , and u channels as independent, should always be avoided. Further, theoretical studies should strive for consistency and completeness by comprehensively treating all crossing-related reaction channels. This will ensure generating optimum dynamic information and physical insight.

ACKNOWLEDGMENTS

The authors acknowledge support provided by the U.S. Department of Energy under Contract No. DE-AS05-79ER10407. One of the authors (S.C.) also acknowledges stimulating discussions with F. Tabakin.

APPENDIX

The four Lorentz- and gauge-invariant amplitudes introduced in Sec. IV are given in terms of the coupling constants and Mandelstam variables s , t , and u , by

$$A_1 = \frac{eg_\Lambda(1+\kappa_p)}{s-m_p^2} + \frac{eg_\Lambda\kappa_\Lambda}{u-m_\Lambda^2} + \frac{eG_\Sigma}{u-m_\Sigma^2} + \frac{\alpha(m_\Lambda+m_p)+\beta t}{t-m_{K^*}^2}, \quad (\text{A1})$$

$$A_2 = \frac{2eg_\Lambda}{(t-m_{K^*}^2)(s-m_p^2)} + \frac{\beta}{t-m_{K^*}^2}, \quad (\text{A2})$$

$$A_3 = \frac{eg_\Lambda\kappa_p}{(s-m_p^2)m_p} + \frac{\alpha-\beta(m_\Lambda-m_p)}{t-m_{K^*}^2}, \quad (\text{A3})$$

$$A_4 = \frac{eg_\Lambda\kappa_\Lambda}{(u-m_\Lambda^2)m_\Lambda} + \frac{2eG_\Sigma}{(u-m_\Sigma^2)(m_\Lambda+m_\Sigma)} + \frac{\alpha+\beta(m_\Lambda-m_p)}{t-m_{K^*}^2}, \quad (\text{A4})$$

with

$$\alpha = \frac{G_V}{m}, \quad \beta = \frac{G_T}{m(m_p + m_\Lambda)}.$$

Using these amplitudes the spin-averaged transition probability appearing in Eq. (48) of Sec. IV is

$$4m_p m_\Lambda \sum_{h\lambda\lambda'} |T_{h\lambda\lambda'}^s|^2 = f(a^2 A_3^2 + b^2 A_4^2) + k A_3 A_4 \\ - (c A_2 + ab A_1) F - d A_2^2 \\ - 4 A_1 (a^2 m_\Lambda A_3 + b^2 m_p A_4), \quad (\text{A5})$$

where

$$F = 4(A_1 - m_p A_3 - m_\Lambda A_4), \quad a = s - m_p^2,$$

$$b = u - m_\Lambda^2, \quad c = a^2 m_\Lambda^2 + b^2 m_p^2 + ab(m_p^2 + m_\Lambda^2 - t),$$

$$d = 2c[(m_p - m_\Lambda)^2 - t],$$

$$f = (m_p + m_\Lambda)^2 - t, \quad k = 2(am_\Lambda - bm_p)^2.$$

¹M. L. Goldberger, in *High Energy Nuclear Physics*, Proceedings of the Sixth Annual Rochester Conference, 1956, edited by J. Ballam *et al.* (Interscience, New York, 1956), p. 1.

²J. Gunson, *J. Math. Phys.* **6**, 827 (1965); **6**, 845 (1965).

³D. Olive, *Phys. Rev.* **135**, B745 (1964).

⁴G. F. Chew, M. L. Golderberg, F. E. Low, and Y. Nambu, *Phys. Rev.* **106**, 1337 (1957).

⁵S. Mandelstam, *Phys. Rev.* **112**, 1344 (1958); **115**, 1741 (1959); **115**, 1752 (1959).

⁶S. C. Frautschi and J. D. Walecka, *Phys. Rev.* **120**, 1486 (1960).

⁷R. E. Cutkosky *et al.*, *Nucl. Phys.* **B102**, 139 (1976).

⁸H. Thom, *Phys. Rev.* **151**, 1322 (1966).

⁹R. A. Adelseck, C. Bennhold, and L. E. Wright, *Phys. Rev. C* **32**, 1681 (1985).

¹⁰M. Alston-Garnjost *et al.*, *Phys. Rev. D* **21**, 1191 (1980).

¹¹W. Cameron *et al.*, *Nucl. Phys.* **B78**, 93 (1974).

¹²E. Eisenhandler *et al.*, *Nucl. Phys.* **B96**, 109 (1975).

¹³V. Girija and F. Tabakin, *Phys. Rev. C* **34**, 1798 (1986).

¹⁴S. S. Hsiao and S. R. Cotanch, *Phys. Rev. C* **28**, 1668 (1983).

¹⁵H. Genzel *et al.*, *Numerical Data and Functional Relationships in Science and Technology*, Vol. 8 of *Landolt-Börnstein* (Springer-Verlag, Berlin, 1973).

¹⁶J. Lowe *et al.*, *Nucl. Phys.* **B209**, 16 (1982).

¹⁷R. L. Workman and H. Fearing, *Phys. Rev. D* **37**, 3117 (1988).

¹⁸J. Cohen, *Phys. Lett.* **153B**, 367 (1985).

¹⁹J. Cohen, *Phys. Lett. B* **192**, 291 (1987).

²⁰A. S. Rosenthal, D. Halderson, K. Hodgkinson, and F. Tabakin, *Ann. Phys. (N.Y.)* (in press).

²¹M. M. Nagels, T. A. Rijken, and J. J. de Swart, *Phys. Rev. D* **15**, 2547 (1977).

²²P. Espigat *et al.*, *Nucl. Phys.* **B162**, 41 (1980).

²³P. H. Timmers, W. A. van der Sanden, J. J. de Swart, *Phys. Rev. D* **29**, 1928 (1984).